Radiation Effects in Defects and Solids, 1989, Vol. 109, pp. 287–292
Reprints available directly from the publisher
Photocopying permitted by license only

A MANY-BODY EMBEDDED ATOM POTENTIAL FOR DESCRIBING EJECTION OF ATOMS FROM SURFACES*

B. J. GARRISON, K. WALZL, M. EL-MAAZAWI, N. WINOGRAD, C. T. REIMANN,† and D. M. DEAVEN‡

Department of Chemistry, The Pennsylvania State University, University Park, PA 16802

(Received 19 September, 1988)

In this paper, we show that many-body interactions are important for describing the energy- and angle-resolved distributions of neutral Rh atoms ejected from keV-ion-bombarded Rh{111}. We compare separate classical-dynamics simulations of the sputtering process assuming either a many-body potential or a pairwise additive potential. The most dramatic difference between the many-body potential and the pair potential is the predicted kinetic energy distributions. The pair-potential kinetic energy distribution peaks at ~ 2 eV, whereas the many-body potential predicts a broader peak at ~ 4 eV, giving much better agreement with experiment. This difference between the model potentials is due to the predicted nature of the attractive interaction in the surface region through which all ejecting particles pass.

The development of many-body interaction potentials to describe the forces among large ensembles of atoms (e.g. solids or liquids) is presently in its infancy. Over the years investigators have sought to find systems and scattering regimes where these types of potential functions may be expressed in a mathematically tractable form. One such process is the ejection of atoms due to 500–5000 eV particle bombardment of solids (i.e., sputtering). In this case atoms are ejected from the solid with a kinetic energy, E_{kin}, distribution which maximizes at 2–10 eV and which decreases as E_{kin}^{-2} up to energies which are a significant fraction of the energy of the incident particle. The complex atomic motion subsequent to the ion-bombardment event is clearly initiated by close encounters between colliding atoms in the solid. These types of interactions may provide an excellent model system for developing an accurate many-body interaction potential.

Since 1960 particle bombardment events have been simulated by computer models which assume pairwise additive potential functions.[1] The simplest approach is to assume that the interactions are purely repulsive and that the collision dynamics can be described by the binary collision approximation where each particle is allowed to interact with only the nearest atom at a given time.[2] On the other hand, we believe that at the energies at which most particles eject, 2–10 eV, simultaneous interactions are not negligible and in fact play a dominant part in controlling the collision dynamics.[3–7] Due to computational restrictions, our full

*We would like to dedicate this article to Don E. Harrison, Jr. a dear friend and colleague, who died recently. Don's first paper on computer simulations of sputtering was published in 1964, long before many of us even dreamed of performing molecular dynamics on real systems. Eleven years ago Don graciously agreed to collaborate and even gave us his computer code—a beginning of an interaction that led to what we believe has been interesting science.

†Current address: Naval Research Laboratory, Washington, DC 20375.
‡Current address: Department of Physics, University of California at Berkeley, Berkeley, CA 94720.

lattice descriptions have thus far been limited to pairwise additive potentials, although attractive interactions have been included.

These potentials have been quite successful at elucidating mechanisms of particle ejection, and at allowing calculation of semiquantitative aspects of the sputtering process.[4]. However, a quantitative comparison between theory and experiment has been hindered by a scarcity of detailed experimental data. The computer simulations using single crystal targets yield direct information concerning the trajectories of ejecting neutral atoms. Early experiments were capable only of examining energy-integrated or angle-integrated neutral distributions from damaged targets or of examining trajectories of secondary ions. The motion of the ions could be detected with high sensitivity but the distributions had to be corrected for the image forces created by the charge.[8] A new method based on the multiphoton resonance ionization of neutral atoms after they have desorbed from the target surface has recently been developed. The technique is capable of measuring the energy- and angle-resolved neutral (EARN) distributions of sputtered atoms[9-11] with sensitivity sufficient to avoid surface damage. These experiments provide the best trajectory data yet available and force a critical test of assumed interaction potentials and scattering dynamics.

In a previous study we described the EARN distributions of Rh atoms ejected from RH{111} with a computer simulation using pairwise additive interaction potentials.[7] Although the overall trends of azimuthal anisotropies and relative intensities of angular peaks were well described, the positions of the peaks and the peak widths in both the polar angle and energy distributions differed between the experimental and calculated results. Variation of the parameters in the potential within physically reasonable bounds did not significantly improve the agreement.

A new model potential for classical dynamical simulations of keV-ion-induced desorption has recently been developed which is based on the embedded atom method (EAM).[12-13] In the EAM, the potential energy of the i-th atom in the lattice is written as $E_i = F(\rho_i = \Sigma_{j \neq i} \rho_{\text{atomic}}(r_{ij})) + 1/2 \Sigma_{j \neq i} \varphi(r_{ij})$. In this expression, r_{ij} is the distance between the i-th and j-th atoms, $\varphi(r_{ij})$ is the potential energy of repulsion between the ion cores of the i-th and j-th atoms, $\rho_{\text{atomic}}(r_{ij})$ is the electron density at the position of the i-th atom due to the j-th atom, and ρ_i is the total electron density at the position of the i-th atom, excluding the electron density provided by the i-th atom itself. The embedding function, F, is a nonlinear function which is taken not to depend on the source of the electron density. Thus, once F is determined, it should be usable in an arbitrary configuration of Rh atoms.

The form of the EAM potential may be derived from density functional theory.[14] With this theory, the embedding energy of the i-th atom is a functional of the self-consistent electron density with the i-th atom removed from the lattice. Two approximations are then made. First, the functional is replaced by a function, and second, the self-consistent electron density is replaced by a homogeneous electron density, the value of which is taken to be the value of the correct density at the position of the i-th atom. Finally, a perturbation theory correction is added taking into account the nonuniformity of the electron density near the atom. The result is an expression with the same form as the EAM. (Another correction term, the hybridization or band energy resulting from the formation of delocalized states in the solid,[15,16] is ignored because it would not reflect the actual band structure in the vicinity of a desorption event.) It should be noted that the EAM and the expression from density functional theory are not rigorously identical, so that the EAM is empirical in nature. Also, an alternative interpretation exists for ρ_i. This parameter may be a measure of local density or coordination of atoms[17] rather than a measure

of local electron density.[12,13] In either interpretation, however, the atomic interactions are the consequence of many-body forces, which is more realistic for metals than the assumption of pairwise additive potentials.[18]

As shown in Figure 1b molecular dynamics calculations using pairwise additive potentials do quite well at reproducing and explaining the angular distributions of Rh atoms ejected from Rh{111}. The question is then, are many-body potentials necessary or is the ejection process dominated by crystal structure and thus the repulsive wall of the potential. Shown in Figure 2 are the measured and calculated (with pairwise additive potentials) angle integrated energy distributions.[7] The curves do not agree nor could they be made to agree with any reasonable variation of the parameters. In addition, the calculated peaks in the polar distributions (Figure 1b) were 5-10° closer to the surface normal than the experimental ones.

A preliminary fit of the embedding function and the core repulsive term was made to the properties of Rh metal in order to determine if the EAM description of the interaction better predicts the EARN data of Rh atoms ejected from Rh{111} than the pair potentials.[18] The most dramatic change in the predicted distributions arises in the angle-integrated energy distributions. As shown in Figure 2 the experimental and calculated distributions using the EAM interaction are in excellent agreement while the calculated distribution using pair potentials is quite different from the experimental curve. The peak in the polar angle distributions as calculated from the EAM are also found to increase by about 10° from those predicted by the pair potentials (Figure 1b). The agreement between the EAM and the experimental energy distributions is better than one could have hoped, and the polar distribution correction is in the right direction.

Is the better agreement fortuitious or is there a sound basis for it? The pair potential description in the surface region has been thought to be inadequate but the detailed data that exposed the nature of the deficiencies was not available. There are several differences between the EAM and pair potentials. First the surface binding energy of the EAM potential is larger (-5.1 eV) than that of the pair potential (-4.1 eV). Of note is that both potentials were fit to the bulk heat of atomization of Rh (5.76 eV). The peak position in the energy distribution is proportional to the binding energy,[19] thus it is logical that the peak in the EAM energy distribution occurs at a higher value than for the pair potential. In addition to the larger binding energy at the equilibrium site, the EAM potential is relatively flat in the attractive portion of the entire surface region. There is more than a 4 eV attraction for the ejecting atom even above a neighboring atom, while the pair potential has only ~ 1 eV overall attraction. Thus particles that eject at more grazing angles will experience a larger attraction to the surface in the EAM potential than in the pair potential. This will tend to make the peak in the energy distribution shift to larger energies, and will also pull the particles away from the surface normal and move the peak in the polar distribution (Figure 1b).

The data actually suggest that the EAM potential is too smooth or planar in the surface region. For amorphous and polycrystalline samples a simple model with a planar surface potential is used to describe the angular distributions.[19,20] The predictions of the model (and the experimental data) give the polar distributions a $\cos^n\theta$ background, especially in the 5-10 eV energy range. Intuitively, this observation suggests that the EAM potentials are too smooth. It is interesting to note that the rather violent keV particle bombardment process is actually yielding insight into the nature of the attractive portion of the metal surface.

Recently the previously developed Rh{111} EAM potential has been employed to model the ejection process from Rh{331}, a stepped surface that consists of

{111} terraces three atoms wide with a one atom step height. In this surface there are atoms that are both more and less coordinated than on the {111} surface. The agreement between the experimental and calculated angular distributions is excellent.[21]

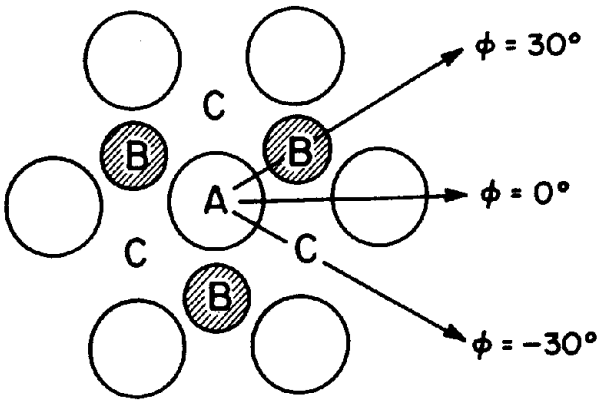

FIGURE 1a Rh{111} crystal face. The open circles are first-layer atoms and the shaded circles represent second-layer atoms. The azimuthal directions of $\phi = -30°$, 0,° and 30° are shown.

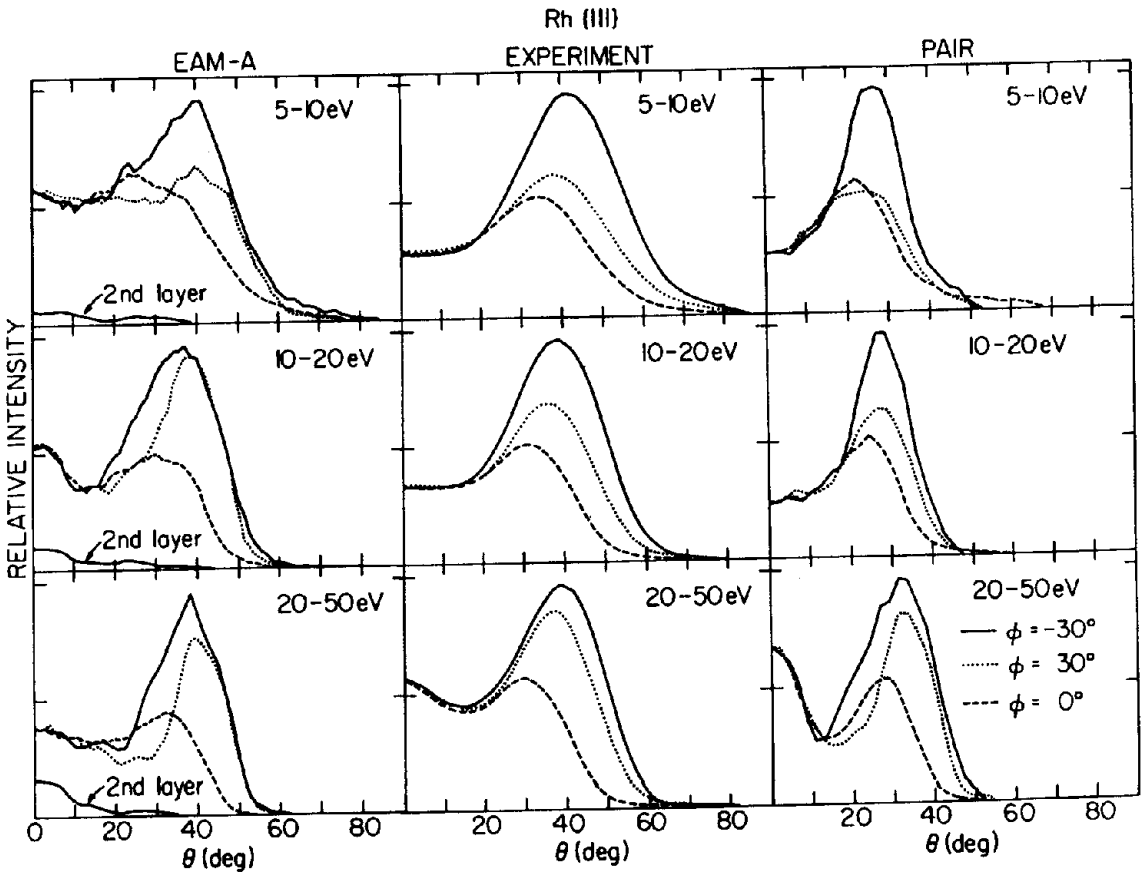

FIGURE 1b Polar angle distributions for various azimuthal angles for fixed secondary kinetic energy of the Rh atoms. In each frame the data are normalized to the $\phi = -30°$ peak intensity. For the calculated data the full width at half maximum (FWHM) of the resolution is 15° in the polar angle. A constant solid angle is used in the histogramming procedure. The experimental resolution is approximately the same. The surface normal corresponds to $\theta = 0°$. The curve marked 2nd layer is the contribution to the polar distribution due to 2nd layer atoms along $\phi = -30°$.

The EAM approach appears to provide a formalism, within realistic potentials, with which describing atomic dynamics can be developed. It should also provide a method for realistically incorporating adsorbates into dynamics simulations. Both of these applications can be considered significant advances, and will help molecular dynamics simulations to continue its contribution to the understanding of technologically important processes.

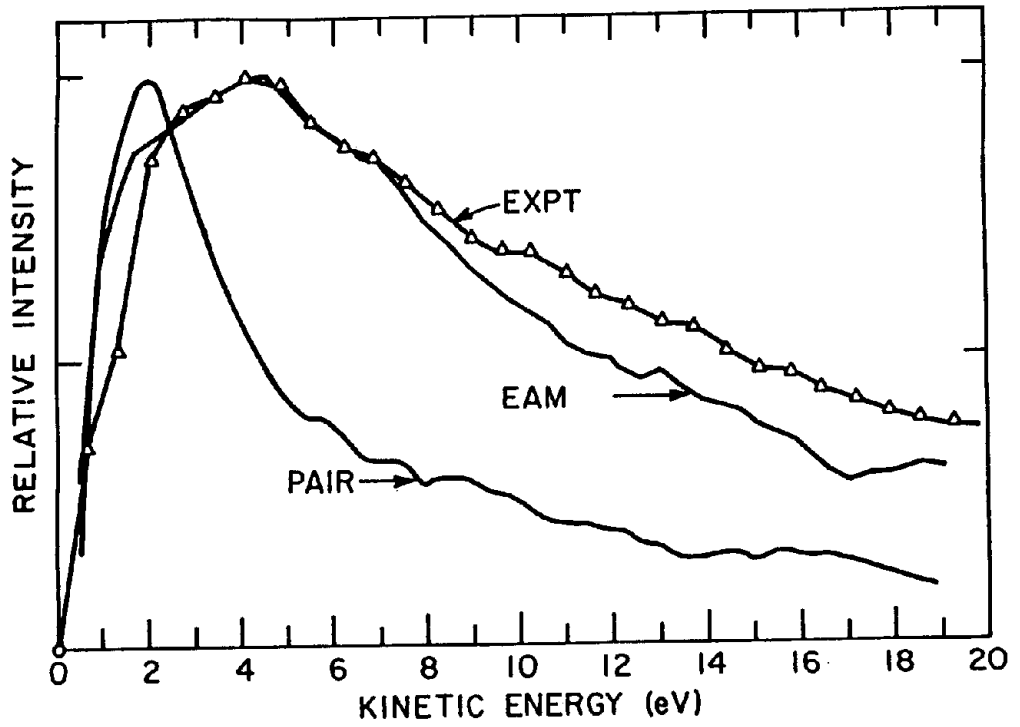

FIGURE 2 Experimental and calculated angle-integrated kinetic energy distributions. In all cases, the curves are peak normalized.

ACKNOWLEDGEMENT

We gratefully acknowledge the financial support of the Office of Naval Research, the National Science Foundation, the IBM Program for the Support of the Materials and Processing Sciences, the Shell Development Corporation, the Camille and Henry Dreyfus Foundation, and the Sloan Foundation. We thank the Pennsylvania State University for a generous grant of computer time.

REFERENCES

1. J. B. Gibson, A. N. Goland, M. Milgram, and G. H. Vineyard, *Phys. Rev.* **120,** 1229 (1960).
2. M. T. Robinsen and I. M. Torrens, *Phys. Rev. B* **9,** 5008 (1974).
3. D. E. Harrison, Jr., J. P. Johnson III, and N. S. Levy, *Appl. Phys. Lett.* **8,** 33 (1966).
4. B. J. Garrison and N. Winograd, *Science* **216,** 805 (1982).
5. M. H. Shapiro, P. K. Haff, T. A. Tombrello, D. E. Harrison, Jr., and R. P. Webb, *Radiat. Eff.* **89,** 243 (1985).
6. D. Y. Lo, M. H. Shapiro, and T. A. Tombrello, *Mater. Res. Soc. Symp. Proc.* **174,** 449 (1987).
7. B. J. Garrison, N. Winograd, C. T. Reimann, and D. E. Harrison, Jr., *Phys. Rev. B* **36,** 3516 (1987).
8. R. A. Gibbs, S. P. Holland, K. E. Foley, B. J. Garrison, and N. Winograd, *Phys. Rev. B* **24,** 6178 (1981).

9. J. P. Baxter, G. A. Schick, J. Singh, P. H. Kobrin, and N. Winograd, *J. Vac. Sci. Technol.* **4**, 1218 (1986).
10. G. A. Schick, J. P. Baxter, J. Singh, P. H. Kobrin, and N. Winograd, in *Secondary Ion Mass-Spectrometry-SIMSV*, Vol. 44 of *Springer Series in Chemical Physics*, A. Benninghoven, R. J. Tolton, D. S. Simons, and H. W. Werner (Eds.) (Springer-Verlag, New York, 1986), p. 90.
11. N. Winograd, P. H. Kobrin, G. A. Schick, J. Singh, J. P. Baxter, and B. J. Garrison, *Surf. Sci.* **176**, 1817 (1986).
12. M. S. Daw and M. I. Baskes, *Phys. Rev. Lett.* **50**, 1285 (1983).
13. M. S. Daw and M. I. Baskes, *Phys. Rev. B* **29**, 6443 (1984).
14. M. Manninen, *Phys. Rev. B.* **34**, 8486 (1986).
15. K. W. Jacobsen, J. K. Nørskov, and M. J. Puska, *Phys. Rev. B* **35**, 7423 (1987).
16. J. K. Nørskov, *Phys. Rev.* **B26**, 2875 (1982).
17. M. W. Finnis and J. E. Sinclair, *Phil. Mag.* **A50**, 45 (1984).
18. B. J. Garrison, N. Winograd, D. M. Deaven, C. T. Reimann, D. Y. Lo, T. A. Tombrello, D. E. Harrison, Jr., and M. H. Shapiro, *Phys. Rev. B* **37**, 7197 (1988).
19. M. W. Thompson, *Phil. Mag.* **18**, 377 (1968).
20. B. J. Garrison, *Nuclear Instru. and Methods* **B17**, 305 (1986).
21. C. T. Reimann, K. Walzl, M. El-Maazawi, N. Winograd, B. J. Garrison and D. M. Deaven, *J. Chem. Phys.* **89**, 2539 (1988).